IMPACT OF TEMPERATURE DEPENDENT HEAT SOURCE AND NONLINEAR RADIATIVE FLOW OF THIRD GRADE FLUID WITH CHEMICAL ASPECTS

TASAWAR HAYAT [a,b], IKRAM ULLAH [a 1], AHMED ALSAEDI [b] and BASHIR AHMAD [b]

[a] Department of Mathematics, Quaid-I-Azam University 45320, Islamabad 44000, Pakistan

[b] Nonlinear Analysis and Applied Mathematics (NAAM) Research Group, Faculty of Science, King Abdulaziz University P. O. Box 80203, Jeddah 21589, Saudi Arabia

Abstract: *This communication explores the magnetohydrodynamic (MHD) flow of third grade fluid bounded by a stretching surface with homogeneous-heterogeneous reactions. Incompressible fluid is electrically conducting in the presence of constant magnetic field. Heat transfer is performed through exponential based space internal heat source, non-linear thermal radiation and convective boundary condition. Nonlinear differential systems are computed by homotopic technique. Intervals of convergence through numerical data and plots are explicitly determined. The dimensionless velocity, temperature and concentration distributions manifesting the characteristics of various influential parameters are addressed. The skin friction coefficient and local Nusselt number are also addressed*. Clearly temperature is enhanced by radiation, temperature ratio and magnetic parameters.

Keywords: *Non-linear thermal radiation; MHD; Exponential based heat source; Homogeneous-heterogeneous reactions.*

1. Introduction

Investigation of non-Newtonian fluids such as paints, cosmetic products, colloidal fluids, suspension fluids, shampoos, blood at low shear rate, ice cream, mud, polymers etc is current area of research for the recent researchers. It is due to their wide uses in engineering and industrial processes. The non-Newtonian fluids in comparison to Newtonian fluids are not easy to analyze. Certainly the diverse behaviors of non-Newtonian fluids cannot be described by Newton's law of viscosity. There is always non-linear link between the shear stresses and shear rate in the case of non-Newtonian fluids. Several models of non-Newtonian fluids for their diverse characteristics are suggested. Mainly such liquids have been classified into three main branches namely the integral, differential and rate types. A simple subclass of differential type fluids is known as second grade describing normal stress only. Note that second grade fluid do not predict shear thinning and shear thickening. Third grade fluids capture shear thinning/shear thickening effects even in one-dimensional steady flow. No doubdt there is a sizeable informations for flows of third grade fluids at present. Few representative studies in this direction can be seen by the attempts $[1-11]$.

The heat transfer in boundary layer flow over a stretching surface has relevance in processes like food processing, cooling of large metallic plat in a bath, glass fiber production, manufacturing of rubber and plastic sheets, wire drawing and many others. Crane $[12]$ was the first who explored the boundary layer flow caused by stretching sheet. Bhattacharyya $[13]$ numerically discussed the heat transfer in boundary layer flow induced by an exponentially stretching surface. Here shooting method is utilized for the solution procedure. Mukhopadhyay $[14]$ analyzed the slip effects in unsteady mixed convective flow and heat transfer over a stretching surface. Hydromagnetic flow and heat transfer in flow of viscoelastic fluid is examined by Turkyilmazoglu $[15]$. Heat transfer and partial slip in MHD flow past a porous shrinking surface explored Zheng et al. $[16]$. Hayat et al. $[17]$ developed the series solutions for heat transfer in

[1]Corresponding author. Tel.: +92 51 90642172.
E-mail address: ikramullah@math.qau.edu.pk (Ikram Ullah)

unsteady flow of Jeffrey fluid over a stretching sheet. Mixed convection flow of viscoelastic fluid over a surface with heat transfer presented by Hayat et al. [18]. Some other related attempts are communicated in [19-28].

In nature there is a wide range of chemical reactions having useful practical applications. Some of the reactions have the capability to proceed moderately or do not react at all without catalyst. In general the contact between the heterogeneous and homogeneous chemical reactions is very complicated. Such reactions link the consumption and production of the reactant materials at distinct rates both within the fluid and on the surface of catalyst. Merkin [29] studied a problem for isothermal homogeneous-heterogeneous reactions in boundary layer flow over a flat plate. The effects of forced convection and homogeneous-hetrogeneous reactions in stagnation point flow was explored by Chaudhary and Merkin [30]. Khan and Pop [31] investigated the flow of viscoelastic fluid over a stretching sheet with homogeneous-hetrogeneous reactions. Flow of Maxwell fluid over a stretching surface with homogeneous-heterogeneous reactions was investigated by Hayat et al. [32]. The characteristics of melting heat and heterogeneous-homogeneous reactions in the flow of viscoelastic fluid was presented by Hayat et al. [33].

Here our prime focus for four aspects. Firstly to consider third grade fluid model with characteristics of MHD. Secondly to utilize the convective heat transport analysis in flow by stretched surface. Thirdly to perform analysis in the presence of homogeneous-heterogeneous reactions. Fourth to develop the series solutions through homotopic technique [34-40]. Sketch of different parameters are presented and discussed in detail. The results of skin friction coefficient and local Nusselt number are also analyzed.

2. Mathematical modeling and constitutive expression

Here we intend the 2D flow of an incompressible third grade fluid over a linear stretching sheet. A constant magnetic field B_0 is implmented parallel to the y axis. Induced magnetic field is not accounted due to the consideration of small Reynolds number. Heat transport is inspected through exponential based space internal heat source and non-linear thermal radiation. A Cartesian coordinate is assumed in such a manner that the $x-$axis is selected along the stretched surface with velocity $U_w = cx$ and $y-$axis is transverse to it. The convectively heated surface is expressed by heat transport coefficient h_f and hot fluid temperature T_f. Aspects of heterogeneous-homogeneous reactions are intended. The isothermal cubic autocatalytic reaction (homogeneous) and the first order reaction (heterogeneous) on the surface of catalyst is demonstrated by [29, 30]:

$$A + 2B \rightarrow 3B, \qquad rate = K_c a b^2, \tag{1}$$

$$A \rightarrow B, \qquad rate = K_s a. \tag{2}$$

The concentrations of the chemical species A and B are a and b while K_c and K_s are the constants. Both the reaction processes are assumed to be isothermal. The governing boundary layer expressions can be put into the form [43-45]:

$$\frac{\partial u}{\partial x} + \frac{\partial v}{\partial y} = 0, \tag{3}$$

$$\begin{aligned} u\frac{\partial u}{\partial x} + v\frac{\partial u}{\partial y} &= \nu\frac{\partial^2 u}{\partial y^2} + \frac{\alpha_1}{\rho}\left(u\frac{\partial^3 u}{\partial x \partial y^2} + \frac{\partial u}{\partial x}\frac{\partial^2 u}{\partial y^2} + 3\frac{\partial u}{\partial y}\frac{\partial^2 u}{\partial x \partial y} + v\frac{\partial^3 u}{\partial y^3} \right) \\ &+ \frac{2\alpha_2}{\rho}\frac{\partial u}{\partial y}\frac{\partial^2 u}{\partial x \partial y} + \frac{6\alpha_3}{\rho}\left(\frac{\partial u}{\partial y}\right)^2 \frac{\partial^2 u}{\partial y^2} - \frac{\sigma B_0^2}{\rho} u, \end{aligned} \tag{4}$$

$$u\frac{\partial T}{\partial x}+v\frac{\partial T}{\partial y}=\alpha_m\frac{\partial^2 T}{\partial y^2}-\frac{1}{(\rho c_p)}\frac{\partial q_r}{\partial y}+Q_0\frac{(T_w-T_\infty)}{\rho c_p}\exp\left(-n\left(\frac{c}{\nu}\right)^{1/2}y\right), \tag{5}$$

$$u\frac{\partial a}{\partial x}+v\frac{\partial a}{\partial y}=D_A\frac{\partial^2 a}{\partial y^2}-K_c ab^2, \tag{6}$$

$$u\frac{\partial b}{\partial x}+v\frac{\partial b}{\partial y}=D_B\frac{\partial^2 b}{\partial y^2}+K_c ab^2. \tag{7}$$

The related boundary conditions are

$$u=U_w=cx,\ v=0,\ -k\frac{\partial T}{\partial y}=h_f(T_f-T),\ D_A\frac{\partial a}{\partial y}=K_s a,\ D_B\frac{\partial b}{\partial y}=-K_s a\ \text{at}\ y=0, \tag{8}$$

$$u\to 0,\ T\to T_\infty,\ a\to a_0,\ b\to 0\ \text{as}\ y\to\infty. \tag{9}$$

In above expressions $(u,\ v)$ corresponds to the velocity components parallel to $x-$ and $y-$directions, μ designates the dynamic viscosity, ν shows the kinematic viscosity, ρ the fluid density, n the exponential index, α_1, α_2 and α_3 the material constants, σ the electrical conductivity, α_m the thermal diffusivity of fluid, c the stretching rate, D_B and D_A the diffusion coefficients of B and A and a_0 the positive dimensionless constant, a and b the concentration of chemical species, T and T_∞ the surface and ambient temperatures respectively. Through Rosseland's approximation the radiative heat flux q_r is [46]:

$$q_r=-\frac{4\sigma^{**}}{3m^{**}}\frac{\partial(T^4)}{\partial y}=-\frac{16\sigma^{**}}{3m^{**}}T^3\frac{\partial T}{\partial y}, \tag{10}$$

in which σ^{**} shows the Stefan-Boltzman and m^{**} designates the coefficient of mean absorption. Invoking Eq. (10) the energy equation can be reduced to the form

$$u\frac{\partial T}{\partial x}+v\frac{\partial T}{\partial y}=\alpha_m\frac{\partial^2 T}{\partial y^2}+\frac{1}{(\rho c_p)}\frac{\partial}{\partial y}\left(\frac{16\sigma^{**}}{3m^{**}}T^3\frac{\partial T}{\partial y}\right)+Q_0\frac{(T_w-T_\infty)}{\rho c_p}\exp\left(-n\left(\frac{c}{\nu}\right)^{1/2}y\right). \tag{11}$$

The transformations are taken in the form

$$\left.\begin{array}{c} u=cxf'(\eta),\ v=-\left(c\nu\right)^{1/2}f(\eta),\ a=a_0 g(\eta),\ b=a_0 h(\eta),\\ T=T_\infty+(T_f-T_\infty)\theta(\eta),\ \eta=\left(\frac{c}{\nu}\right)^{1/2}y. \end{array}\right\} \tag{12}$$

Invoking above definitions, the continuity eq. (1) is now identically satisfied and eqs. $(4)-(9)$ and (11) become

$$f'''+ff''-f'^2+\beta_1\left(2f'f'''-ff''''\right)+\left(3\beta_1+2\beta_2\right)f''^2+6\varepsilon_1\varepsilon_2 f'''f''^2-M^2 f'=0, \tag{13}$$

$$\left.\begin{array}{c} (1+\frac{4}{3}Rd)+\frac{4}{3}Rd[(\theta_w-1)^3(3\theta'^2\theta^2+\theta^3\theta'')+3(\theta_w-1)^2(2\theta'^2\theta+\theta^2\theta'')\\ +3(\theta_w-1)(\theta'^2+\theta\theta'')]+\Pr f\theta'+\Pr\delta\exp(-\eta)=0, \end{array}\right\} \tag{14}$$

$$\frac{1}{Sc}g''+fg'-K_1 gh^2=0, \tag{15}$$

$$\frac{\delta}{Sc}h''+fh'+K_1 gh^2=0, \tag{16}$$

$$f=0,\ f'=1,\ \theta'=-\gamma(1-\theta),\ g'=K_2 g,\ \delta h'=-K_2 h \text{ at } \eta=0, \tag{17}$$

$$f'\to 0,\ \theta\to 0\ g\to 1,\ h\to 0 \text{ as } \eta\to\infty. \tag{18}$$

Where $\beta_1,\ \beta_2$ and ε_1 are the material parameters for third grade fluid, ε_2 is the local Reynolds number, M represents the magnetic parameter, δ the internal heat source parameter, Rd the radiation parameter, $\Pr$ stands for the Prandtl number, γ the Biot number, θ_w the temperature ratio parameter, K_1 denotes the strength of homogeneous reaction parameter, δ the diffusion coefficient ratio, K_2 the strength of heterogeneous reaction, Sc the Schmidt number and prime designates differentiation with respect to η. These quantities are expressed as follows:

$$\left.\begin{aligned}&\beta_1=\tfrac{c\alpha_1}{\mu},\ \beta_2=\tfrac{c\alpha_2}{\mu},\ \varepsilon_1=\tfrac{c\alpha_3}{\mu},\ M^2=\tfrac{\sigma B_0^2}{\rho c},\ \Pr=\tfrac{\nu}{\alpha_m},\ K_1=\tfrac{K_c a_0^2}{c},\ Rd=\tfrac{4\sigma^{**}T_\infty^3}{m^{**}k}\\ &\delta=\tfrac{Q_0}{c\rho c_p},\ \theta_w=\tfrac{T_w}{T_\infty},\ \varepsilon_2=\tfrac{cx^2}{\nu},\ K_2=\tfrac{K_s}{D_A}\sqrt{\tfrac{\nu}{c}},\ Sc=\tfrac{\nu}{D_A},\ \delta=\tfrac{D_B}{D_A},\ \text{and } \gamma=\tfrac{h_f}{k}\sqrt{\tfrac{\nu}{c}}.\end{aligned}\right\} \tag{19}$$

Here comparable size is presumed for the coefficients of diffusion of chemical species B and A. This fact provides us to establish further supposition that the coefficients of diffusion D_A and D_B are same i.e. $\delta=1$ and thus:

$$g(\eta)+h(\eta)=1. \tag{20}$$

Now eqs. (13) and (14) give

$$\frac{1}{Sc}g''+fg'-K_1 g(1-g)^2=0, \tag{21}$$

and the corresponding boundary conditions are

$$g'(0)=K_2 g(0),\quad g(\infty)\to 1. \tag{22}$$

Expressions for velocity gradient (C_{f_x}) and temperature gradient (Nu_x) are

$$C_{f_x}=\frac{2\tau_w}{\rho U_w^2},\ Nu_x=\frac{xq_w}{k\left(T_f-T_\infty\right)}+(q_r)_w, \tag{23}$$

where

$$\tau_w=\left[\mu\frac{\partial u}{\partial y}+\alpha_1\left(u\frac{\partial^2 u}{\partial x\partial y}+2\frac{\partial u}{\partial x}\frac{\partial u}{\partial y}+\upsilon\frac{\partial^2 u}{\partial y^2}\right)+2\alpha_3\left(\frac{\partial u}{\partial y}\right)^3\right]_{y=0},\ q_w=-k\left(\frac{\partial T}{\partial y}\right)_{y=0}. \tag{24}$$

The dimensionless form of Eq. (23) gives

$$\left.\begin{aligned}&\left(\mathrm{Re}\right)^{1/2}C_{f_x}=\left(f''+\beta_1\left(3f'f''-ff'''\right)+2\varepsilon_1\varepsilon_2 f''^3\right)_{\eta=0},\\ &\left(\mathrm{Re}\right)^{-1/2}Nu_x=-(1+\tfrac{4}{3}Rd(1+(\theta_w-1)\theta_w)^3\theta'(0),\end{aligned}\right\} \tag{25}$$

where Re is the Reynolds number defined by $\mathrm{Re}=U_w x/\nu$.

3. Series solutions and convergence

The initial guesses and operators are given below:

$$f_0(\eta)=1-e^{-\eta},\quad \theta_0(\eta)=\frac{\gamma}{1+\gamma}e^{-\eta},\quad g_0(\eta)=1-\frac{1}{2}e^{-K_2\eta}, \tag{26}$$

$$\mathbf{L}_f=f'''-f',\qquad \mathbf{L}_\theta=\theta''-\theta,\qquad \mathbf{L}_g=g''-g, \tag{27}$$

$$\mathbf{L}_f\left[C_1+C_2e^{\eta}+C_3e^{-\eta}\right]=0,\ \mathbf{L}_\theta\left[C_4e^{\eta}+C_5e^{-\eta}\right]=0,\ \mathbf{L}_g\left[C_6e^{\eta}+C_7e^{-\eta}\right]=0, \tag{28}$$

in which the constants $C_i \ \ (i=1-7)$ are defined by

$$\left.\begin{array}{c} C_2 = C_4 = C_6 = 0,\ C_3 = \frac{\partial f_m^*(\eta)}{\partial \eta}|_{\eta=0},\ C_1 = -C_3 - f_m^*(0), \\ C_5 = \frac{1}{1+\gamma}\frac{\partial \theta_m^*(\eta)}{\partial \eta}|_{\eta=0} - \frac{\gamma}{1+\gamma}\theta_m^*(0),\ C_7 = \frac{1}{1+K_2}[\frac{\partial g_m^*(\eta)}{\partial \eta}|_{\eta=0} - K_2 g_m^*(0)]. \end{array}\right\} \tag{29}$$

In homotopic solutions, the rate of deformation and convergence region highly depend upon $\hbar_f$, $\hbar_\theta$ and $\hbar_g$. For such interest, the $\hbar$-curves have been plotted in Fig. 1 at 16-th order of deformations. Such curves provide the admissible ranges of these auxiliary parameters. It is clear from this fig. 1 that the suitable ranges of these parameters are $[-1.0,-0.1]$, $[-1.4,-0.4]$ and $[-1.1,-0.2]$. Besides that the series solutions are convergent in all region of η when $\hbar_f = -0.4 = \hbar_\theta = \hbar_g$. Table 1 shows that 30 th order of approximations up to 4 decimal places are adequate for good agreement regarding convergence.

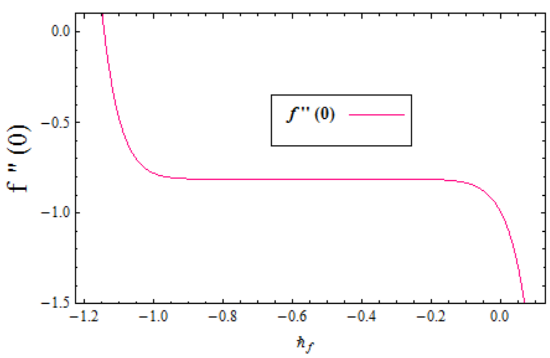

Fig. 1: The ħ-curve for $f(\eta)$

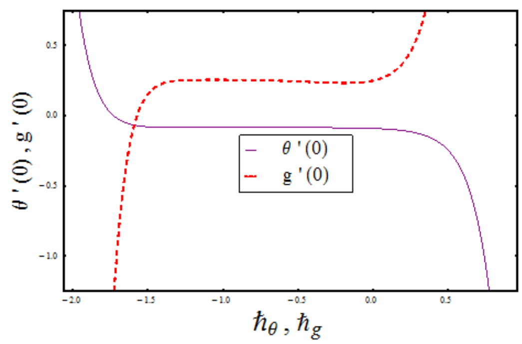

Fig. 2: The ħ-curves for $\theta(\eta)$ and $g(\eta)$

Table 1: **Convergence of homotopic solutions when** $Rd = 0.4 = \delta$, $\theta_w = 0.3$, $\varepsilon_1 = \varepsilon_2 = 0.2 = M = \gamma$, $\beta_1 = 0.1 = \beta_2$, $\Pr = 1.0$, $K_1 = 0.5 = K_2$, $Sc = 0.9$

Order of approximations	$f''(0)$	$-\theta'(0)$	$g'(0)$
1	0.8550	0.0895	0.2410
10	0.8126	0.0855	0.2394
20	0.8127	0.0851	0.2516
30	0.8127	0.0850	0.2550
40	0.8127	0.0850	0.2550
45	0.8127	0.0850	0.2550
50	0.8127	0.0850	0.2550
60	0.8127	0.0850	0.2550

4. Results and Discussion

This portion focuses for the impact of distinct influential parameters on the dimensionless velocity $f'(\eta)$, temperature $\theta(\eta)$ and concentration $g(\eta)$ profiles. These outcomes are interpreted via graphs in the Figs. $(3)-(14)$. The consequences of magnetic parameter M on the velocity distribution $f'(\eta)$ can be seen in Fig. 3. For larger magnetic parameter M the velocity field reduces close to the surface and it vanishes away from the surface. It is quite obvious because larger magnetic parameter corresponds to enhancement of Lorentz forces thereby reducing the velocity profile $f'(\eta)$. Fig. 4 investigates the impact of material parameter β_1 on $f'(\eta)$. It is seen that velocity distribution increases when we enlarge β_1. The characteristics of material parameter β_2 on the velocity field is sketched in Fig. 5. It is concluded that higher values of β_2 corresponds to an enhancement in the fluid velocity$\cdot$ In fact higher values of material parameter tend to enhance the normal stresses and it reduces the viscous forces which lead to increase the fluid velocity. Fig. 6 declared the aspect of Rd on $\theta(\eta)$. Here bigger values of Rd augments the thermal field. As expected heat is produced due to radiation process in the working fluid so thermal distribution enhances. Fig. 7 presents the variations in magnetic parameter M on the temperature distribution $\theta(\eta)$. It is well known established fact that the magnetic field intensity tends to create drag force which restricts the fluid motion and heats up the fluid. There is rise in the temperature and thickness of thermal boundary layer. Note that the case $M=0$ corresponds to hydrodynamic flow situation. Feature of δ on $\theta(\eta)$ is pointed out in Fig. 8. It is figure out that thermal field is enhances via δ. Fig. 9 illustrates the consequences of Biot number γ on the temperature filed $\theta(\eta)$. It is noticed that both temperature and thermal layer thickness are increasing functions of Biot number $\cdot$ Fig. 10 depicts the change of temperature in response to change in the θ_w. Both thermal field and associated layer thickness are enhance when θ_w is enlarged. Fig. 11 portrays the influence of Prandtl number $\Pr$ on the temperature profile $\theta(\eta)$. Fluids of higher Prandtl have minimum thermal conductivities so that heat can spread away from the plate slower than for smaller $\Pr$ fluids. Hence rise in Prandtl number substantially decreases the temperature and thickness of thermal boundary layer. Larger strength of homogeneous reaction K_1 shows a reduction in concentration distribution $g(\eta)$ (see Fig. 12). Fig. 13 explores the impacts of strength of the heterogeneous reaction K_2 on the concentration profile $g(\eta)$ There is an increases in concentration field $g(\eta)$ for larger values of K_2. Fig. 14 shows the impact of Biot number γ and Prandtl number $\Pr$ on Nusselt number. It is examined that by increasing γ and $\Pr$ the Nusselt number enhances. Numerical data of skin friction coefficient $-(\mathrm{Re})^{1/2} C_{f_x}$ for pertinent flow parameters including ε_1, ε_2, M, β_1, β_2, $\Pr$ and γ are presented in tab. 2. It is found that the coefficient of skin friction increases for higher values of $\Pr$ and M whereas opposite effect is observed for γ.

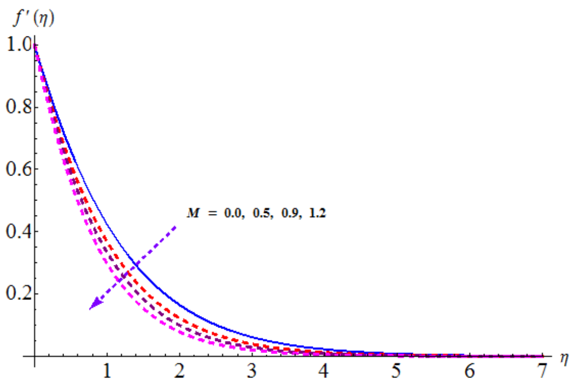

Fig. 3. Impact of M on $f'(\eta)$.

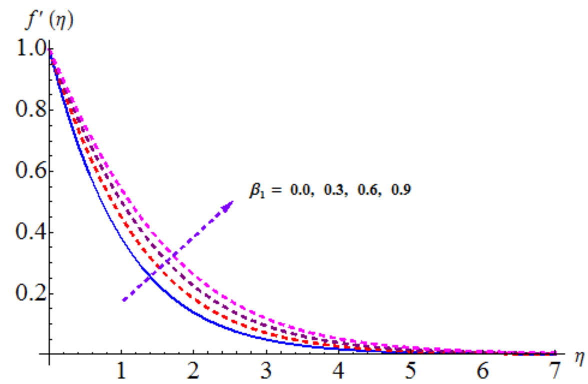

Fig. 4. Impact of β_1 on $f'(\eta)$.

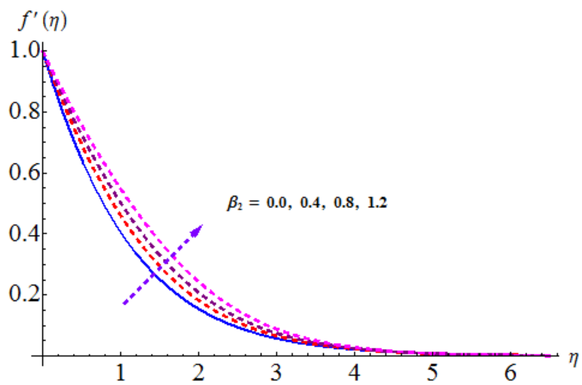

Fig. 5. Impact of β_2 on $f'(\eta)$.

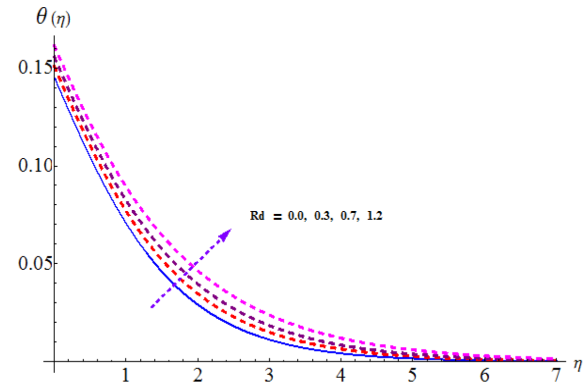

Fig. 6. Impact of Rd on $\theta(\eta)$.

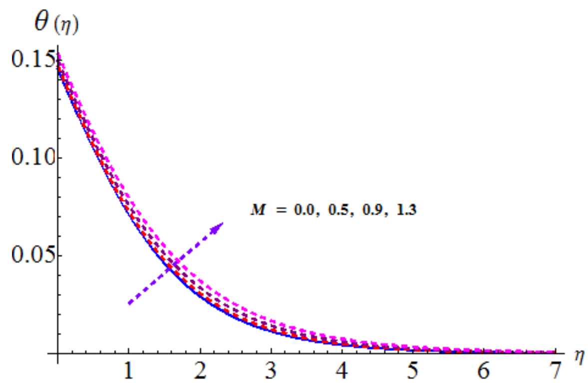

Fig. 7. Impact of M on $\theta(\eta)$.

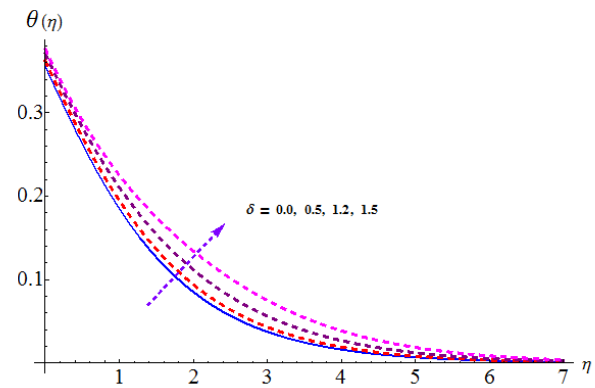

Fig. 8. Impact of δ on $\theta(\eta)$.

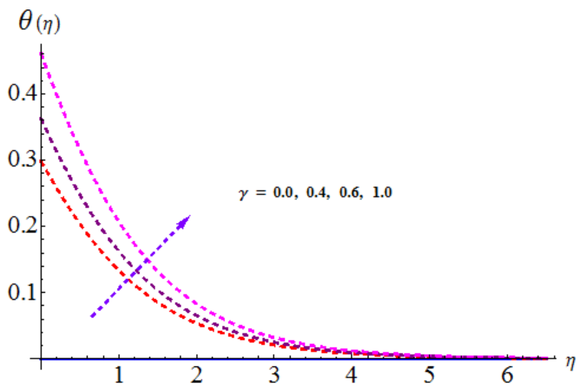

Fig. 9. Impact of γ on θ(η).

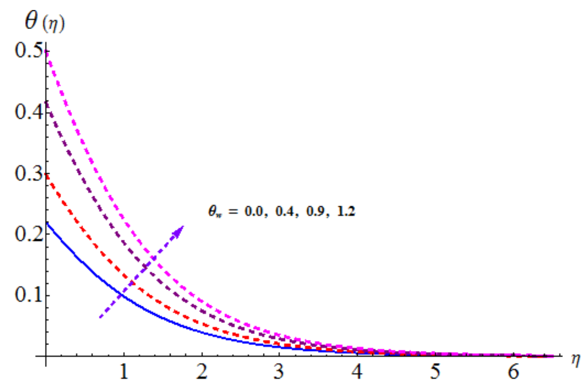

Fig. 10. Impact of θ_w on θ(η).

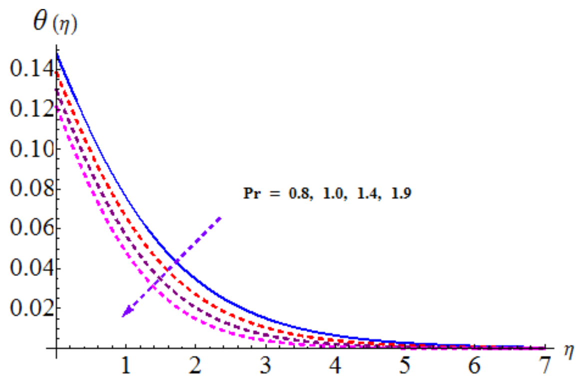

Fig. 11. Impact of Pr on θ(η).

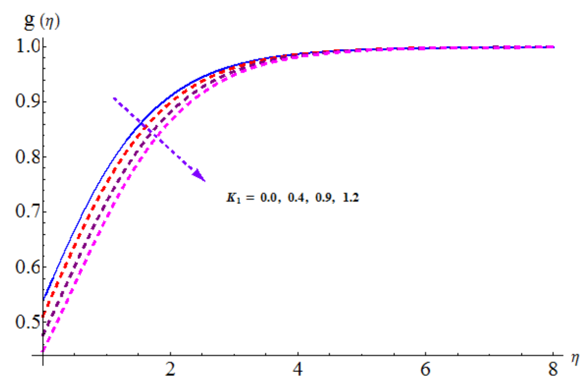

Fig. 12. Impact of K_1 on g(η).

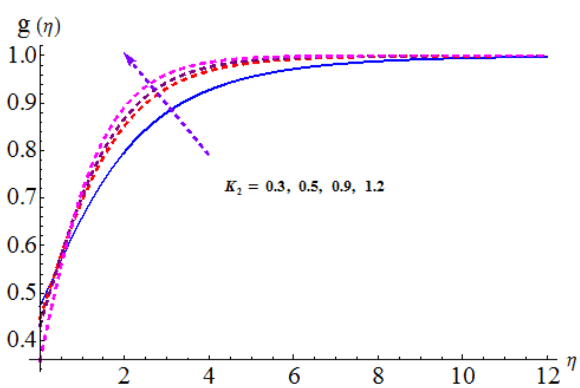

Fig. 13. Impact of K_2 on g(η).

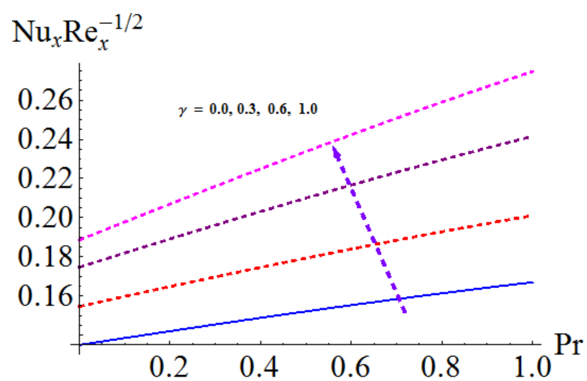

Fig. 14. Impacts of Pr and γ on Nusselt number.

Table 2: Numerical estimations of drag force $-(\mathrm{Re})^{1/2} C_{fx}$ for various values of ε_1, ε_2, M, β_1 and β_2 when $Rd = 0.4 = \delta$, $\theta_w = 0.3$, $\Pr = 0.9$, $\gamma = 0.1$, $K_1 = 0.5 = K_2$ and $Sc = 0.9$.

ϵ_1	ϵ_2	β_1	β_2	M	$-Re_x^{\frac{1}{2}} C_{fx}$
0.2	0.2	0.1	0.1	0.2	1.0835
0.3					1.1067
0.6					1.1274
0.2	0.0	0.1	0.1	0.2	1.0835
	0.3				1.1067
	0.7				1.1339
0.2	0.1	0.0	0.1	0.2	0.9814
		0.2			1.2064
		0.4			1.3964
0.2	0.2	0.1	0.0	0.2	1.1539
			0.2		1.0041
			0.5		0.9244
0.2	0.2	0.1	0.1	0.0	1.0779
				0.4	1.1616
				0.8	1.3858

5. Conclusions

Homogeneous-heterogeneous reactions in magnetohydrodynamic (MHD) flow of third grade fluid over a starching sheet are explored. Main results are reported below.

- The characteristics of material parameters β_1 and β_2 has similar effects on the velocity field.
- Increasing values of M show opposite behavior for the velocity and temperature fields.
- An enhancement in convective parameter γ shows an increment in temperature field.
- Temperature field is enhancing function of δ, Rd and θ_w.
- The heterogeneous and homogeneous reactions strengths show an opposite behavior on concentration field.
- Magnitude of skin friction coefficient is increasing functions of β_1 and M.
- Local Nusselt number represents the opposite behavior for higher values of M and $\Pr$.

References

[1] Okoya, S. S., Flow, thermal criticality and transition of a reactive third-grade fluid in a pipe with Reynolds model viscosity, *Journal of Hydrodynamics*, Ser. B, *28* (2016), 1, pp. 84-94

[2] Li, S. X., Jian, Y. J., Xie, Z. Y., Liu, Q. S., Li, F. Q., Rotating electro-osmatic flow of third grade fluids between two microparallel plates, *Collids and Surfaces A*, *470* (2015), pp. 240-247

[3] Aziz, T., Mahomed, F. M., Auyb, M. Mason, D. P., Nonlinear time-dependent flow models of third grade fluids: A conditional symmetry approch, *International Journal of Non-Linear Mechanics*, *54* (2013), pp. 55-65

[4] Abdelhameed, M., Varnhorn, W., Hashim, I., Roslan, R., The unsteady flow of third grade fluid caused by the periodic motion of an infinite wall with transpiration, *Alexandria Engineering*

Journal, *54* (2015), 4, pp. 1233-1241
[5] Sinha, A., MHD flow and heat transfer of third order fluid in a porous channel with stretching wall: Application to hemodynamics, *Alexandria Engineering Journal*, *54* (2015), 4, pp. 1243-1252
[6] Abbasbandy, S., Hayat, T., Mahomed, F. M., Ellahi, R., On comparison of exact and series solutions for thin film flow of a third grade fluid, *International Journal for Numerical Methods in Fluids*, *61* (2009), pp. 987-994
[7] Hussain, T., Hayat, T., Shehzad, S. A., Alsaedi, A., Chen, B., A model of solar radiation and Joule heating in flow of third grade nanofluid, *Zeitschrift für Naturforschung A*, *70* (2015), 3, pp. 177-184
[8] Sahoo B., Poncet S., Flow and heat transfer of a third grade fluid past an exponentially stretching sheet with partial slip boundary condition, *International Journal of Heat and Mass Transfer*, *54* (2011), pp. 5010–5019
[9] Sahoo B., Do Y., Effects of slip on sheet-driven flow and heat transfer of a third grade fluid past a stretching sheet, *International Communications in Heat and Mass Transfer*, *37* (2010), pp. 1064–1071
[10] Sahoo B., Effects of slip on sheet-driven flow and heat transfer of a non-Newtonian fluid past a stretching sheet, *Computers and Mathematics with Applications*, *61* (2011), pp. 1442–1456
[11] Hayat, T., Ullah, I., Muhammad, T., Alsaedi, A., A revised model for stretched flow of third grade fluid subject to magneto nanoparticles and convective condition, *Journal of Molecular Liquids*, *230* (2017), pp. 608-615

[12] Crane, L. J., Flow past a stretching plate, *Zeitschrift für angewandte Mathematik und Physik ZAMP*, *21* (1970), 4, pp. 645-647
[13] Bhattacharyya, K., Boundary layer flow and heat transfer over an exponentially shrinking sheet, *Chinese Physics Letters*, *28* (2011), pp. 074701
[14] Mukhopadhyay, S., Effects of slip on unsteady mixed convective flow and heat transfer past a stretching surface, *Chinese Physics Letters*, *27* (2010), pp. 124401
[15] Turkyilmazoglu, M., Multiple solutions of hydromagnetic permeable flow and heat transfer for viscoelastic fluid, *Journal of Thermophysics and Heat Transfer*, *25* (2011), pp. 595-605
[16] Zheng, L., Niu, J., Zhang, X., Gao, Y., MHD flow and heat transfer over a porous shrinking surface with velocity slip and temperature jump, *Mathematical and Computer Modelling*, *56* (2012), 5-6, pp. 133-144
[17] Hayat, T., Ullah, I., Alsaedi A., Ahmad, B., Radiative flow of Carreau liquid in presence of Newtonian heating and chemical reaction, *Results in Physics*, *7* (2017), pp. 715-722
[18] Hayat, T., Anwar, M. S., Farooq, M., Alsaedi, A, Mixed convection flow of viscoelastic fluid by a stretching cylinder with heat transfer, *PLoS One*, *10* (2015), pp. e0118815
[19] Hayat, T., Ullah, I., Alsaedi A., Ahmad, B., Modeling tangent hyperbolic nanoliquid flow with heat and mass flux conditions, *The European Physical Journal Plus*, *132* (2017), pp. 112

[20] Rehman K. U., Malik M. Y., Salahuddin T., Naseer M., Dual stratified mixed convection flow of Eyring-Powell fluid over an inclined stretching cylinder with heat generation/absorption effect, *AIP Advances*, *6* (2016), pp. 075112
[21] Hayat, T., Ullah, I., Alsaedi, A., Farooq, M., MHD flow of Powell-Eyring nanofluid over a non-linear stretching sheet with variable thickness, *Results in Physics*, *7* (2017), pp. 189-196

[22] Bibi M., Rehman K. U., Malik M. Y., Tahir M., Numerical study of unsteady Williamson fluid flow and heat transfer in the presence of MHD through a permeable stretching surface, *The European Physical Journal Plus, 133* (2018), pp. 154

[23] Hayat, T., Ullah, I., Muhammad, T., and Alsaedi, A., Magnetohydrodynamic (MHD) three-dimensional flow of second grade nanofluid by a convectively heated exponentially stretching surface, *Journal of Molecular Liquids, 220* (2016), pp. 1004-1012

[24] Rehman K. U., Khan A. A., Malik M. Y., Makinde O. D., Thermophysical aspects of stagnation point magnetonanofluid flow yields by an inclined stretching cylindrical surface: a non-Newtonian fluid model, *Journal of the Brazilian Society of Mechanical Sciences and Engineering 39* (2017), pp. 3669-3682

[25] Hayat, T., Ullah, I., Muhammad, T., Alsaedi, A., Radiative three-dimensional flow with Soret and Dufour effects, *International Journal of Mechanical Sciences, 133* (2017), pp. 829-837

[26] Hayat, T., Ullah, I., Muhammad, T., Asghar, S., MHD stagnation-point flow of Sisko liquid with melting heat transfer and heat generation/absorption, *Journal of Thermal Sciences and Engineering Applications,* (2018) pp. 051015

[27] Rehman K. U., Khan A. A., Malik M. Y., Magneto-nanofluid numerical modelling of chemically reactive Eyring-Powell fluid flow towards both flat and cylindrical an inclined surfaces: A comparative study, *AIP Advances 7* (2017), pp. 065103

[28] Rehman K. U., Malik M. Y., Bilal S., Bibi M., Numerical analysis for MHD thermal and solutal stratified stagnation point flow of Powell-Eyring fluid induced by cylindrical surface with dual convection and heat generation effects, *Results in physics, 7* (2017), pp. 482-492

[29] Merkin, J. H., A model for isothermal homogeneous-heterogeneous reactions in boundary layer flow, *Mathematical and Computer Modelling, 24* (1996), pp. 125-136

[30] Chaudhary, M. A., Merkin, J. H., A simple isothermal model for homogeneous-heterogeneous reactions in boundary layer flow: I. Equal diffusivities, *Fluid Dynamics Research, 16* (1995), 6, pp. 311-333

[31] Khan, W. A., Pop, I., Effects of homogeneous-heterogeneous reactions on the viscoelastic fluid towards a stretching sheet, *Journal of Heat Transfer | ASME DC, 134* (2012), pp. 064506

[32] Hayat, T., Imtiaz, M., Almezal, S., Modeling and analysis for three-dimensional flow with homogeneous-heterogeneous reactions, *AIP Advances, 5* (2015), pp. 107209

[33] Hayat, T., Hussain, Z., Farooq, M. Alsaedi, A., Effects of homogeneous and heterogeneous reactions and melting heat in the viscoelastic fluid flow, *Journal of Molecular Liquids, 215* (2016), pp. 749-755

[34] Liao, S. J., Homotopy analysis method in nonlinear differential equations, Springer & Higher Education Press, Heidelberg, 2012.

[35] Turkyilmazoglu, M., Solution of the Thomas-Fermi equation with a convergent approach, *Communications in Nonlinear Science and Numerical Simulation, 17* (2012), pp. 4097-4103

[36] Abbasbandy, S., Hayat, T., Alsaedi, A. Rashidi, M. M., Numerical and analytical solutions for Falkner-Skan flow of MHD Oldroyd-B fluid, *International Journal of Numerical Methods for Heat and Fluid Flow, 24* (2014), pp. 390-401

[37] Hayat, T., Ullah, I., Alsaedi, A., Waqas, M., Ahmad, B., Three-dimensional mixed convection flow of Sisko nanoliquid, *International Journal of Mechanical Sciences, 133* (2017), pp. 273-282

[38] Ullah I., Waqas M., Hayat T., Alsaedi A. and Khan M. I., Thermally radiated squeezed

flow of magneto-nanofluid between two parallel disks with chemical reaction, J. *Therm. Anal. Calorim.*, (2018) Doi.org/10.1007/s10973-018-7482-6.

[39] Rashidi, M. M., Ashraf, M., Rostami, B., Rastegari, M. T., Bashir, S., Mixed convection boundary layer flow of micro polar fluid towards a heated shrinking sheet by homotopy analysis method, *Thermal science, 20* (2016), pp. 21-34

[40] S. Ahmad, Khan, M. I., Khan, M. W. A., Tufail, A., Hayat, T., Ahmed. A., Impact of arrhenius activation energy in viscoelastic nanomaterial flow subject to binary chemical reaction and nonlinear mixed convection, *Thermal Science*, (2018) pp. 212-212

[41] Hayat, T., Ullah, I., Muhammad, T., Asghar, S., Flow of magneto Williamson nanoliquid towards stretching sheet with variable thickness and double stratification, *Radiation Physics Chemistry* (2018), doi.org/10.1016/j.radphyschem.2018.07.006

[42] Sui, J., Zheng, L., Zhang, X., Chen, G., Mixed convection heat transfer in power law fluids over a moving conveyor along an inclined plate, *International Journal of Heat and Mass Transfer, 85* (2015), pp. 1023-1033

[43] Hayat, T., Ullah, I., Ahmed, B., Alsaedi A., MHD mixed convection flow of third grade liquid subject to non-linear thermal radiation and convective condition, *Results Physics, 7* (2017), pp. 2804-2811

[44] Zaigham Zia, Q. M., Ullah, I., Waqas, M., Alsaedi, A., Hayat, T., Cross diffusion and exponential space dependent heat source impacts in radiated three-dimensional (3D) flow of Casson fluid by heated surface, *Results in Physics, 8* (2018), pp. 1275–1282

[45] Hayat, T., Ullah, I., Alsaedi, A., Ahmed, B., Numerical simulation for homogeneous–heterogeneous reactions in flow of Sisko fluid, *Journal of the Brazilian Society of Mechanical Sciences and Engineering, 40* (2018), pp. 73

[46] Hayat, T., Ullah, I., Alsaedi, A., Ahmed, B., Simultaneous effects of non-linear mixed convection and radiative flow due to Riga-plate with double stratification, *Journal of Heat Transfer,* 140 (2018), pp. 102008